NASA TECHNICAL NOTE

NASA TN D-4067

NASA TN D-4067

PROJECTILE SIZE EFFECTS ON HYPERVELOCITY IMPACT CRATERS IN ALUMINUM

by B. Pat Denardo, James L. Summers, and C. Robert Nysmith

Ames Research Center

Moffett Field, Calif.

NATIONAL AERONAUTICS AND SPACE ADMINISTRATION • WASHINGTON, D. C. • JULY 1967

NASA TN D-4067

PROJECTILE SIZE EFFECTS ON HYPERVELOCITY IMPACT CRATERS IN ALUMINUM

By B. Pat Denardo, James L. Summers,
and C. Robert Nysmith

Ames Research Center
Moffett Field, Calif.

NATIONAL AERONAUTICS AND SPACE ADMINISTRATION

For sale by the Clearinghouse for Federal Scientific and Technical Information
Springfield, Virginia 22151 – CFSTI price $3.00

PROJECTILE SIZE EFFECTS ON HYPERVELOCITY IMPACT CRATERS IN ALUMINUM

By B. Pat Denardo, James L. Summers,
and C. Robert Nysmith

Ames Research Center

SUMMARY

Hard aluminum (2017-T4) spheres with diameters, d, of 1/16, 1/8, 1/4, and 1/2 inch were launched, in sabots, into thick targets of hard (2024-T4) and soft (1100-0) aluminum at velocities up to 28,000 ft/sec.

Momentum transferred to the target during impact was measured by means of a simple ballistic pendulum to which the target was attached. The ratio of target momentum to projectile momentum increased with increasing projectile diameter, clearly demonstrating a projectile-size effect.

The effects of the projectile size were determined quantitatively from the depth, P, of the crater and its diameter, volume, and shape. In the hypervelocity regime, the dimensionless penetration, P/d, varied with projectile diameter to the 1/18 power for the conditions of this experiment.

INTRODUCTION

Measurements of momentum transferred from projectile to target during impact indicate there are projectile-size effects for hypervelocity impacts (ref. 1). To deduce the effects of projectile size on crater dimensions from momentum measurements, it was assumed that the crater shape and ejecta velocity were independent of the projectile size. It was concluded that the impact penetration depth varied as the 19/18 power of projectile diameter. The assumptions used to obtain this result seemed reasonable, but it was desired to examine them experimentally, and that is the motivation for the present investigation. In addition, the velocity range of the earlier data was extended.

Thick targets of hard and soft aluminum were impacted by hard-aluminum spheres of from 1/16- to 1/2-inch diameter at velocities up to 28,140 ft/sec. The physical dimensions of the craters formed (including penetration, diameter, and volume) and the momentum transferred to the target were measured. These measurements are presented and discussed herein.

SYMBOLS

D	diameter of crater measured in plane of undisturbed surface, in.
D_i	idealized crater diameter with replaced detached lip, in. (see text)
d	projectile diameter, in. or ft (when used with a fractional exponent)
E	projectile energy at impact, ft-lb
M	initial mass of ballistic pendulum including target, lb
ΔM	target mass loss due to cratering, lb
m	mass of projectile, lb
M_e	mass of ejecta ($\Delta M + m$), lb
P	penetration (maximum depth of crater) measured from undisturbed surface, in.
U	crater volume measured from undisturbed surface, in.
U_i	idealized crater volume with replaced detached lip, $in.^3$ (see sketch (a))
U_p	projectile volume, $in.^3$
V	velocity of pendulum immediately after impact, ft/sec
V_e	average axial ejecta velocity, ft/sec
v	velocity of projectile at impact, ft/sec

EXPERIMENTAL PROCEDURE

The projectiles used were 2017-T4 aluminum alloy spheres with diameters of 1/16, 1/8, 1/4, and 1/2 inch. They were launched, in sabots, into free flight by light-gas guns or standard powder-gas guns, depending upon the desired impact velocity.

Thick targets of two aluminum alloys were used: 2024-T4 with a Brinell hardness of nominally 120 and 1100-0 with a hardness of nominally 23. Target thickness and width were at least four times the penetration and crater diameter, respectively. Although no special effort was made to scale the target size directly with the projectile size, certain targets did scale dimensionally. However, no differences in crater measurements were noted between the scaled and unscaled targets. The targets were securely attached to the front face of a ballistic pendulum for measuring the momentum during impact. Since

the momentum varied by a factor of nearly 1500, it was necessary to use pendulums of widely different sizes in order to maintain a sufficient degree of accuracy. An analysis of all parameters involved in the measurement of momentum transfer indicates these measurements are accurate to within 2 percent.

All crater dimensions were measured with the undisturbed target face as the reference plane. Penetration depths were measured with a specially adapted dial indicator. Crater diameters were measured with a Gaertner filar-micrometer microscope. Four readings from edge to edge of each crater were made, then averaged, to give the diameter. Crater volumes were measured by two methods, depending upon the smoothness of the crater. On smooth craters, a plaster casting was first made of the cavity. Then, profile tracings of several views (appropriately enlarged) of the casting were made on an optical comparator. Moments of inertia of each tracing were measured with a mechanical integrator, and the volume was determined from the average for each crater. On pitted, rough craters, where castings were not feasible, volumes were measured with a buret using a liquid composed of water and a wetting agent. Both methods of measuring the volume were used on a number of smooth craters for comparison purposes. In all cases, the maximum variation was less than 3 percent.

The test program was conducted in two free-flight ballistic ranges to accommodate the various projectile sizes. In both ranges, there were spark-shadowgraph stations for accurately determining the projectile's velocity and structural integrity.

A more detailed discussion of the data-reduction techniques can be found in reference 2.

DISCUSSION OF RESULTS

Table I is a compilation of the pertinent data of this investigation.

Momentum transferred to the target is shown in figure 1 as a function of impact velocity for hard-aluminum spheres impacting hard- and soft-aluminum targets. These plots are presented in order to illustrate the effect of projectile size on the cratering process and to portray the effects of velocity on momentum ratio. The magnitude of the projectile-size effect will be further defined subsequently through the analysis of the crater parameters. The shape of the

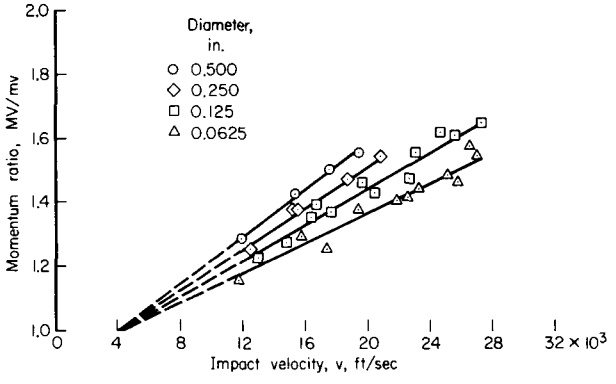

(a) 1100-0 aluminum targets.

Figure 1.- Momentum imparted to target as a function of velocity for four projectile sizes.

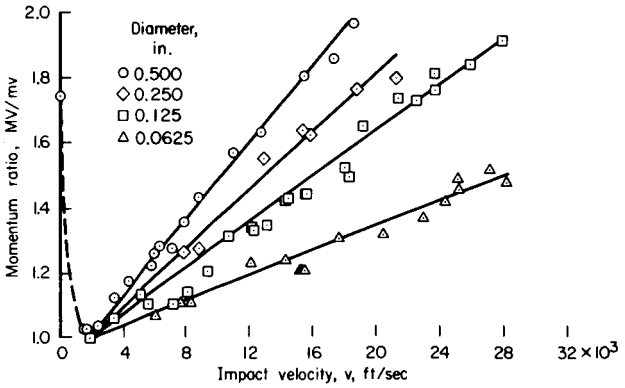

(b) 2024-T4 aluminum targets.

Figure 1.- Concluded.

curves in figure 1(b) is similar to that obtained for polyethylene projectiles impacting hard-aluminum targets, as reported in reference 2. These characteristic shapes reveal several prominent features. At essentially 0 ft/sec (drop tests at 11 ft/sec), the momentum ratio is simply 1 plus the coefficient of restitution. As the velocity of impact increases, the ratio diminishes, reaching a minimum value of 1.0, then rises systematically with velocity. The velocity corresponding to the minimum value of momentum transfer, the threshold velocity, marks the onset of both target mass-loss and projectile-size effects. At this unique point the impact is pseudo-inelastic and no effects of projectile size are apparent. It is interesting that in 2024-T4 targets this threshold velocity is 3100 ft/sec for polyethylene (ref. 2) and 1800 ft/sec for aluminum projectiles. One would expect this difference since the onset of mass loss occurs at lower velocities as the projectile density increases. In the soft 1100-0 targets the threshold velocity is approximately 4000 ft/sec for the aluminum projectiles.

The momentum transfer during impact shows there is a projectile-size effect. In order to determine the extent of associated dimensional changes, a crater parametric analysis was performed. The crater measurements P, D, and U were defined as shown in sketch (a). There was an obvious difference

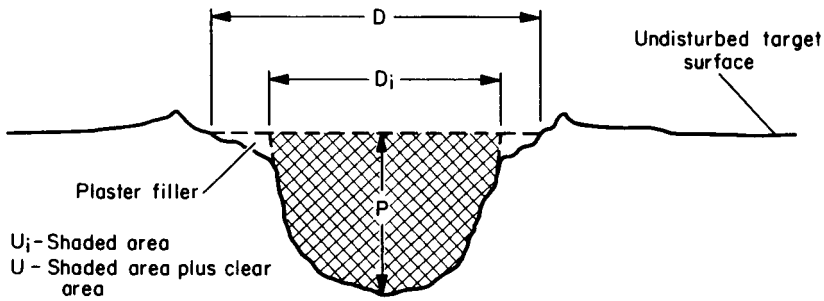

Sketch (a) Typical crater in 2024-T4 at high velocities.

between the results for the hard and soft targets because the craters in the hard targets had detached lips whereas those in the soft targets did not. It was therefore decided to "replace" the lip with a plaster filler (see sketch (a)) and to analyze the data based upon the measurements of the resulting "idealized" crater. The parameters affected were crater diameter, volume, and shape of the hard targets. Of course, the soft targets were unaffected since their lips remain attached in this velocity range.

All hard-target data above a velocity of 13,800 ft/sec were analyzed in the fashion just described and are shown in figures 2 to 5.[1] Best

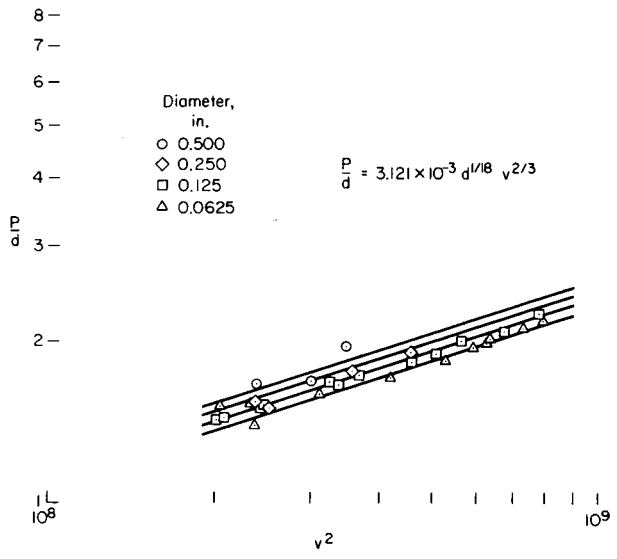

Figure 2.- Penetration as a function of velocity squared for 2024-T4.

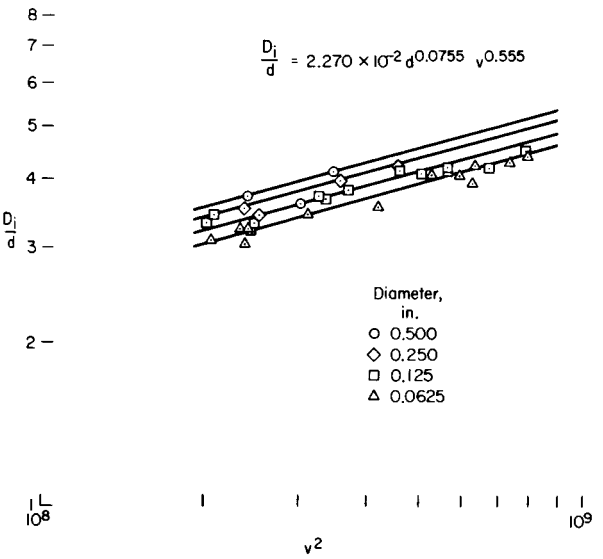

Figure 3.- Diameter as a function of velocity squared for 2024-T4.

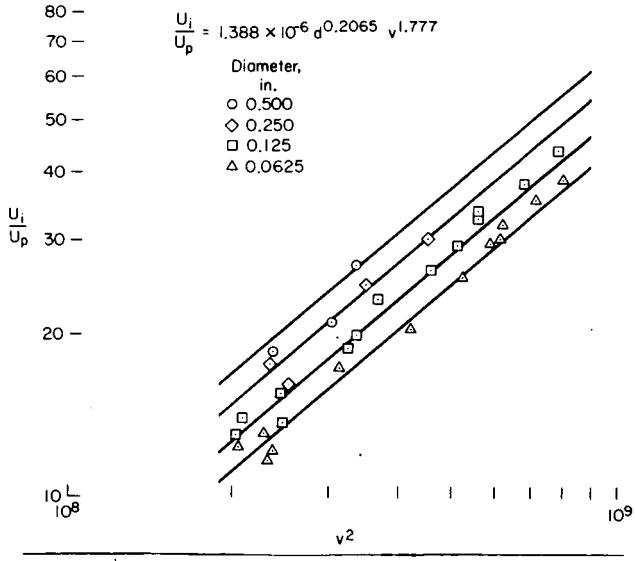

Figure 4.- Volume as a function of velocity squared for 2024-T4.

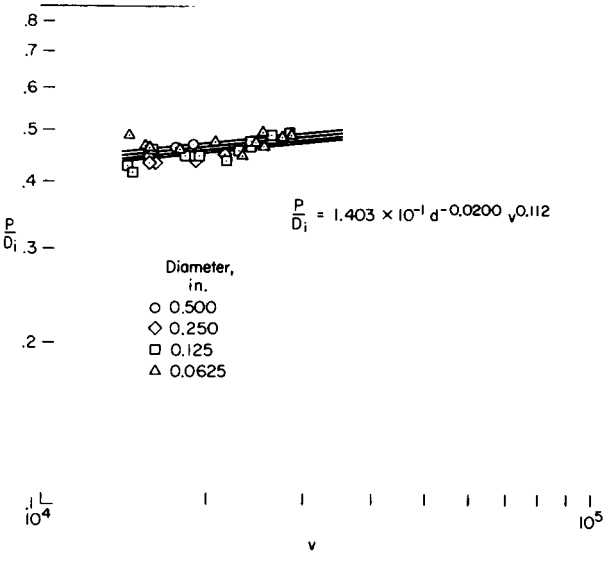

Figure 5.- Crater shape as a function of velocity for 2024-T4.

[1]The velocity range covered in this experiment encompasses a transition region of impact as well as the hypervelocity region (ref. 3). It has been shown that for 1/3 caliber polyethylene projectiles impacting hard-aluminum targets up to a velocity of 37,000 ft/sec, the hypervelocity regime of impact (i.e., where P/d is proportional to $v^{2/3}$) commences at a velocity of 25,500 ft/sec (ref. 4), which corresponds to an impact pressure of 0.57 Mb. For the materials of the present investigation, the velocity corresponding to this pressure is 15,900 ft/sec, if shape effects are ignored. Unpublished data indicate that this velocity will be somewhat lower, perhaps 13,800 ft/sec, for spherical projectiles.

fits to the data were obtained based on the fact that for cavities with similar profiles, the volume is

$$U_i \sim PD_i^2 \tag{1}$$

and the projectile volume is

$$U_p \sim d^3$$

Thus

$$\frac{U_i}{U_p} \sim \frac{PD_i^2}{d^3} \tag{2}$$

but

$$\frac{PD_i^2}{d^3} = \left(\frac{P}{d}\right)^2 \left(\frac{D_i}{d}\right) \left(\frac{D_i}{P}\right) \tag{3}$$

and so

$$\frac{U_i}{U_p} = k \left(\frac{P}{d}\right)^2 \left(\frac{D_i}{d}\right) \left(\frac{D_i}{P}\right) \tag{4}$$

(These equations also apply to the soft targets, but the subscript i would be dropped since there is no lip detachment involved.)

We now have all the crater parameters (penetration, diameter, volume, and shape) contained in a single equation. Best fits to the penetration, diameter, and volume data (figs. 2 to 4) were determined based on the following conditions:

(1) The exponents of both the diameter and velocity were required to be independent of scale, and

(2) Data sets having the most points and the most consistent alinement of points were given the most consideration.

The fit to the crater shape as shown in figure 5 was then derived from equation (4).

It is interesting that the lip detachment is a function of the projectile diameter. The ratios of the actual-to-idealized diameter and volume are plotted versus projectile diameter in figure 6. These points represent the average of all values at velocities above 13,800 ft/sec. It appears that there is no lip detachment for projectile diameters below 1/16 inch. It is coincidental that a 1/16-inch projectile diameter was the smallest chosen for this experiment. An examination of individual craters shows that practically all the lip is attached for the 1/16-inch data, but detached for the 1/2-inch data.

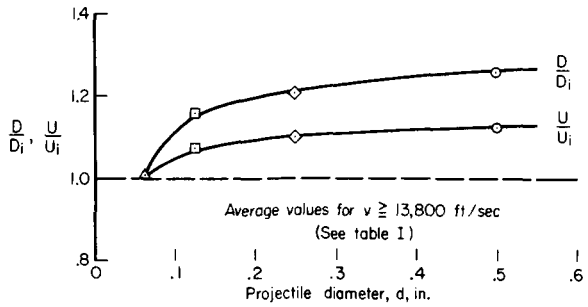

Figure 6.- Idealized diameter and volume variations with projectile diameter for 2024-T4 targets.

The soft-target data were analyzed in the same manner as the hard-target data. Crater parameter plots are shown in figures 7 to 10.

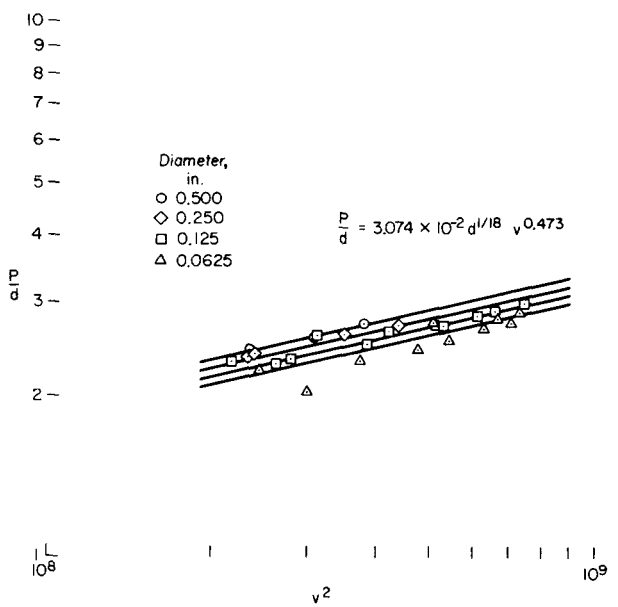

Figure 7.- Penetration as a function of velocity squared for 1100-0.

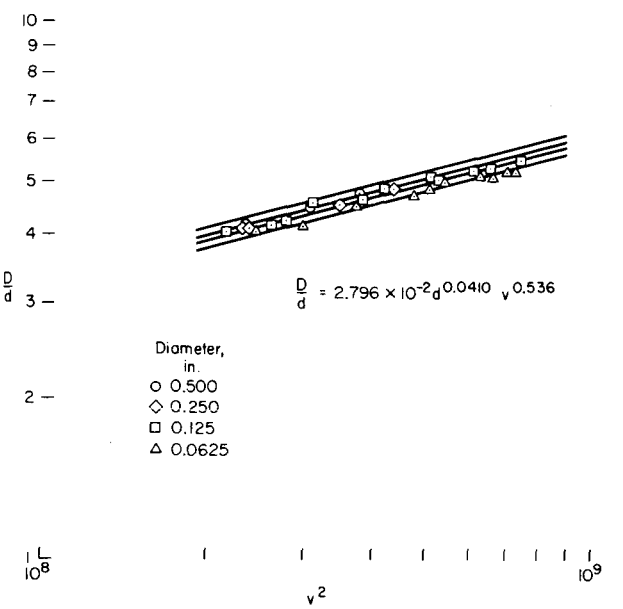

Figure 8.- Diameter as a function of velocity squared for 1100-0.

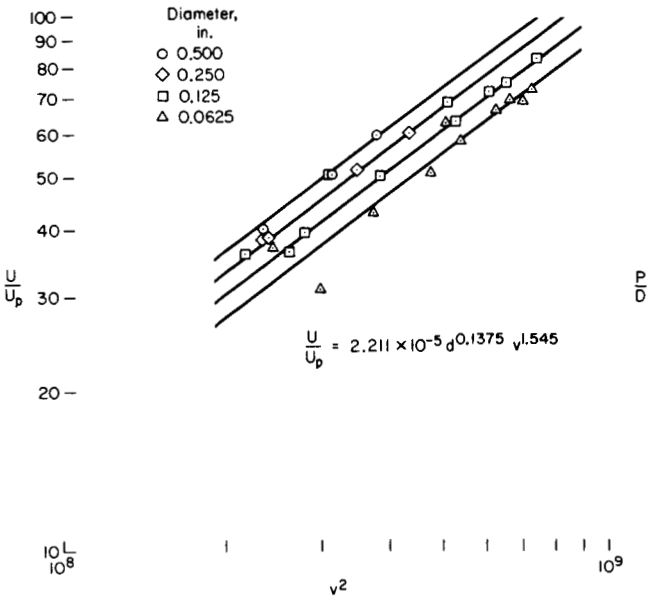

Figure 9.- Volume as a function of velocity squared for 1100-0.

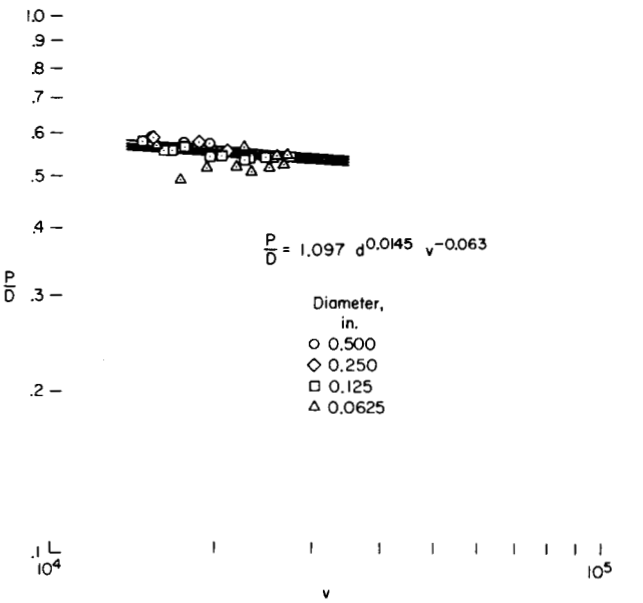

Figure 10.- Crater shape as a function of velocity for 1100-0.

Equations defining each crater parameter for both hard- and soft-aluminum targets are given below for the hypervelocity regime.

2024-T4 aluminum targets:

$$\frac{P}{d} = 3.121 \times 10^{-3} d^{1/18} v^{2/3} \tag{5}$$

$$\frac{D_i}{d} = 2.270 \times 10^{-2} d^{0.0755} v^{0.555} \tag{6}$$

$$\frac{U_i}{U_p} = 1.388 \times 10^{-6} d^{0.2065} v^{1.777} \tag{7}$$

$$\frac{P}{D_i} = 1.403 \times 10^{-1} d^{-0.0200} v^{0.112} \tag{8}$$

1100-0 aluminum targets:

$$\frac{P}{d} = 3.074 \times 10^{-2} d^{1/18} v^{0.473} \tag{9}$$

$$\frac{D}{d} = 2.796 \times 10^{-2} d^{0.0410} v^{0.536} \tag{10}$$

$$\frac{U}{U_p} = 2.211\times10^{-5} d^{0.1375} v^{1.545} \tag{11}$$

$$\frac{P}{D} = 1.097\ d^{0.0145} v^{-0.063} \tag{12}$$

In figure 11, the average values for the crater parameters above a velocity of 13,800 ft/sec, normalized for velocity by applying the velocity exponents just determined, have been plotted against projectile diameter. These plots enable one to assess the accuracy of the fits applied to the data and to comprehend better the effect of projectile size on cratering. The solid lines represent the size effect in equations (5) through (12). In figure 11(a), the fits are adequate except for the volume ratio for the

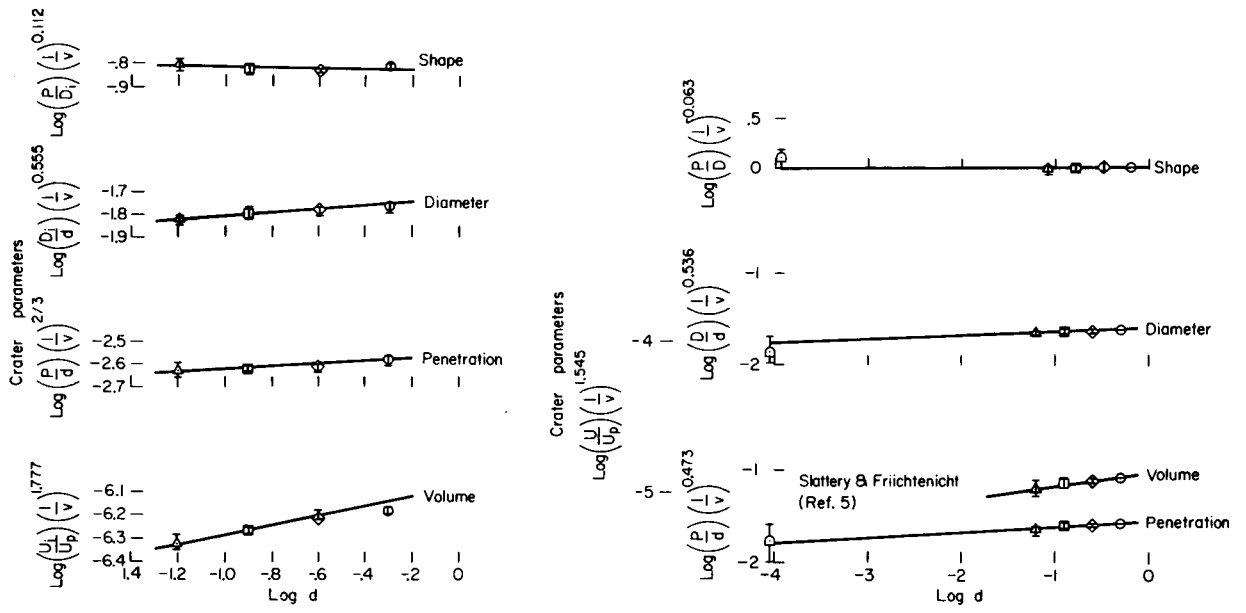

(a) 2024-T4 aluminum targets.

(b) 1100-0 aluminum targets.

Figure 11.- Crater parameters as functions of projectile diameter at velocities above 13,800 ft/sec.

1/2-inch-diameter projectiles. It is reasonable and necessary for this point to be low. No effort was made to duplicate surface pitting in the plaster lips; therefore, the volume, U_i, would be low, and hence, the ratio, U_i/U_p, would also be low. In figure 11(b), the diameter scale has been extended four orders of magnitude to accommodate the data of Slattery and Friichtenicht (ref. 5). These data were obtained with micron-size aluminum spheres impacting soft-aluminum targets. The crater dimensions measured were penetration depth and diameter. The points on the plot represent the average of their data in the velocity range of interest here, from 13,800 to 28,140 ft/sec. The points are plotted at the average diameter of the spheres used in their experiment. As can be seen, agreement in the penetration ratio is excellent.

The penetration for both target materials is compared in figure 12. For the conditions of this experiment, at velocities above about 15,000 ft/sec, the penetration, P/d, varies with the projectile diameter to the 1/18 power and with the impact velocity to the 2/3 power for 2024-T4 and 0.473 power for 1100-0. The scatter in the 2024-T4 data between 4,000 and 10,000 ft/sec is due to marked pitting of the crater bottom in this velocity range, a characteristic of hard targets (ref. 2). The bend in the 2024-T4 curve between 10,000 and 15,000 ft/sec lends credence to the supposition that the hypervelocity regime commences at 13,800 ft/sec.

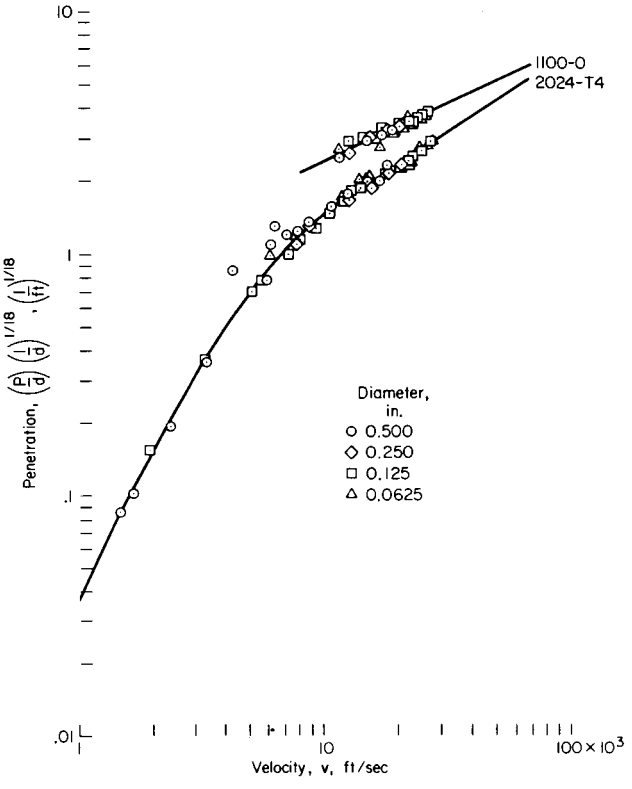

Figure 12.- Correlated penetration versus impact velocity.

It is evident that the assumptions used earlier (ref. 1) (i.e., the crater shape, P/D, and the ejecta velocity, V_e, must be independent of the projectile size) to obtain the size effect from momentum data were not precisely valid. Although they seemed reasonable, closer examination shows a size effect in the crater shape parameter P/D derived from measurements of crater depth, diameter, and volume (figs. 5 and 10). The data show that the two parameters, penetration and diameter, are affected differently for changes in projectile diameter.

The average axial component of ejecta velocity, V_e, may be determined from the conservation of momentum

$$MV = mv + M_e V_e \tag{13}$$

or

$$V_e = \frac{MV - mv}{M_e} \tag{14}$$

It was found that V_e contained a large amount of scatter, as did M_e; however, when the two are combined in $M_e V_e$, smoothing takes place. Nevertheless, a size effect can definitely be noted in V_e; but the scatter cannot be well enough defined to assess the size effect accurately.

CONCLUDING REMARKS

The effects of projectile size on cratering are small but definitely not insignificant. As a matter of fact, an estimate of penetration damage of a micron-sized particle, based on laboratory experiments with 1/2-inch-diameter projectiles, would be almost 70 percent too large if size effects were disregarded. This result is corroborated by Slattery and Friichtenicht (ref. 5) for soft-aluminum targets. The agreement between macro- and microparticle penetration, with allowance for size effects described herein, up to velocities of 28,000 ft/sec is remarkable. In view of this very recent work by Slattery and Friichtenicht, the 1/18-power law for scaling penetration has been experimentally extended over a diameter range of four orders of magnitude, or a mass range of twelve orders of magnitude.

The accepted variation of penetration with velocity in the hypervelocity regime(P/d is a function of $v^{2/3}$) for 2024-T4 targets is substantiated. For the 1100-0 targets, this exponent drops to less than 1/2. It is reasonable to expect that both these values will diminish with increasing velocity as more of the energy goes into heating and vaporization of target material.

Ames Research Center
National Aeronautics and Space Administration
Moffett Field, Calif., 94035, May 3, 1967
124-09-02-07-00-21

REFERENCES

1. Denardo, B. Pat; and Nysmith, C. Robert: Momentum Transfer and Cratering Phenomena Associated With the Impact of Aluminum Spheres Into Thick Aluminum Targets at Velocities to 24,000 Feet Per Second. AGARDograph 87, vol. I. Gordon and Breach, Science Publishers, New York.

2. Denardo, B. Pat: Measurements of Momentum Transfer From Plastic Projectiles to Massive Aluminum Targets at Speeds up to 25,600 Feet Per Second. NASA TN D-1210, 1962.

3. Summers, James L.: Investigation of High-Speed Impact: Regions of Impact and Impact at Oblique Angles. NASA TN D-94, 1959.

4. Denardo, B. Pat: Penetration of Polyethylene Into Semi-Infinite 2024-T351 Aluminum up to Velocities of 37,000 Feet Per Second. NASA TN D-3369, 1966.

5. Slattery, J. C.; and Friichtenicht, J. F.: Experimental Research on Hypervelocity Cratering by Microscopic Particles. TRW Systems Rep. 03246-6001-R000 (Contract NASw-1116, Final Rep.), November 1966.

TABLE I.- SUMMARY OF PERTINENT DATA

Round	Target material	M, lb	V, ft/sec	MV, lb-sec	m, lb	v, ft/sec	mv, lb-sec	E, ft-lb	$\frac{MV}{mv}$	ΔM, lb	d, in.	P, in.	D, in.	U, $in.^3$	D_1, in.	U_1, $in.^3$
MS-159	2024-T4	217.32	0.5260	3.556	66.157×10^{-4}	11,000	2.264	12.45×10^{3}	1.571	3.000×10^{-2}	0.500	0.668	1.90	0.6284		
MS-174		226.92	.6059	4.277	66.175	12,740	2.622	16.70	1.631	5.600		.740	1.95	.8969		
MS-621		198.83	.9299	5.751	66.320	15,465	3.190	24.67	1.803	8.941		.831	2.30	1.324	1.875	1.220
MS-622		210.09	1.0157	6.637	66.270	17,350	3.576	31.02	1.856	10.17		.839	2.35	1.617	1.810	1.397
MS-627		209.83	1.1550	7.538	66.188	18,630	3.835	35.72	1.966	13.34		.982	2.57	1.957	2.080	1.733
P-188		217.08	.1544	1.043	66.241	4,305	.8870	1.909	1.176	.3086		.360	.80	.0635		
P-192		217.55	.2777	1.879	66.193	7,170	1.476	5.291	1.273	1.213		.506	1.35	.241		
P-194		217.42	.2514	1.700	66.181	6,430	1.324	4.257	1.284	1.273		.547	1.35	.214		
P-195		130.41	.1247	.5058	66.124	2,370	.4874	.5776	1.038	.000		.081	.65	.018		
P-200		217.42	.3252	2.199	66.190	7,885	1.623	6.399	1.355	1.607		.523	1.45	.313		
P-201		130.00	.1936	.7828	66.212	3,380	.6961	1.176	1.125	.0606		.150	.80	.037		
P-205		116.22	.0977	.353	66.208	1,665	.3429	.2855	1.03	.000		.043	.42	.003455		
P-207		116.22	.0867	.313	66.151	1,480	.3045	.2253	1.03	.000		.036	.40	.002685		
P-215		216.75	.2332	1.572	66.173	6,065	1.248	3.785	1.260	.9513		.460	1.25	.189		
P-216		217.30	.3840	2.595	66.164	8,815	1.814	7.995	1.431	2.337		.571	1.60	.402		
P-217		217.30	.2210	1.494	66.210	5,935	1.222	3.626	1.223	.5765		.323	1.15	.149		
MS-623	1100-0	227.39	.6373	4.587	66.283	15,295	3.153	24.11	1.429	*		1.226	2.10	2.630		
MS-624		218.22	.4629	3.142	66.290	11,830	2.439	14.43	1.288	2.223		1.052	1.80	1.667		
MS-625		225.46	.7746	5.432	66.188	17,520	3.607	31.60	1.506	*		1.294	2.25	3.323		
MS-626		226.37	.8865	6.242	66.166	19,470	4.007	39.01	1.558	*		1.372	2.39	3.922		
MS-290	2024-T4	19.77	1.0500	.6457	8.230	15,405	.3943	3.037	1.638	.9325	.250	.385	1.055	.162	.889	.146
MS-367		20.26	.8156	.5140	8.230	12,940	.3312	2.143	1.552	.6371		.339	.900	.1025		
MS-368		19.75	1.0743	.6600	8.219	15,885	.4061	3.225	1.625	.7518		.375	1.020	.137	.865	.128
P-232		20.21	.4071	.2559	8.285	7,915	.2025	.8814	1.264	.124		.222	.570	.031		
P-233		18.89	.4915	.2888	8.225	8,845	.2263	1.001	1.276	.140		.265	.600	.037		
MS-612		42.77	.6373	.8478	8.230	18,790	.4810	4.519	1.763	1.300		.438	1.250	.226	1.000	.201
MS-613		52.31	.6021	.9797	8.230	21,280	.5447	5.796	1.799	1.498		.479	1.280	.278	1.060	.250
MS-614	1100-0	45.78	.2808	.3998	8.221	12,425	.3177	1.974	1.258	.2313		.531	.905	.223		
MS-615		53.75	.3247	.5428	8.254	15,250	.3915	2.985	1.386	.3865		.596	1.025	.314		
MS-616		61.79	.2839	.5456	8.214	15,475	.3954	3.059	1.380	.4592		.604	1.025	.318		
MS-619		61.77	.3677	.7065	8.230	18,700	.4787	4.476	1.476	.4134		.657	1.140	.424		
MS-620		69.79	.3806	.8262	8.223	20,875	.5339	5.573	1.547	*		.680	1.220	.496		
SP-532	2024-T4	7.8311	.3623	.08825	1.032	18,035	.05789	.5220	1.524	.0959	.125	.210	.500	.0210	.467	.0195
SP-534		7.8232	.2971	.07229	1.034	15,595	.05016	.3911	1.441	.0661		.188	.450	.0158	.409	.0156
SP-537		7.8331	.2977	.07253	1.030	15,705	.05031	.3951	1.442	.0672		.189	.430	.01494	.416	.0142
SP-632		6.0831	.2770	.05241	1.032	12,175	.03908	.2379	1.341	.0351		.160	.400	.01035		
SP-635		6.0485	.3493	.06572	1.027	14,410	.04603	.3316	1.428	.0714		.180	.430	.01464	.434	.0144
SP-636		6.0465	.3012	.05665	1.030	13,150	.04213	.2770	1.345	.0529		.177	.400	.01213		
SP-637		6.0593	.2787	.05253	1.030	12,320	.03947	.2431	1.331	.0386		.162	.380	.009723		
SP-638		7.8413	.3607	.08797	1.030	18,355	.05880	.5396	1.496	.0990		.207	.485	.0204	.463	.0205
SP-699		3.3616	.6182	.06464	1.021	14,210	.04513	.3206	1.432	7.67×10^{-4}		.179	.465	.0143	.416	.0136
SP-700		3.3558	.4343	.04533	1.030	10,755	.03446	.1853	1.315	3.13		.144	.335	.00732		
P-455		3.3444	.3515	.03656	1.030	9,470	.03034	.1437	1.205	2.0		.125	.305	.005175		
P-456		3.3459	.2856	.02972	1.032	8,105	.02602	.1054	1.142	1.7		.111	.280	.00403		
P-457		3.2460	.2555	.02580	1.030	7,290	.02336	.08515	1.104	.972		.097	.235	.00300		
P-458		3.1881	.1895	.01879	1.030	5,160	.01653	.04265	1.137	.258		.068	.200	.00136		
P-460		3.0787	.0646	.00619	1.030	1,940	.006215	.006028	.996	.055		.015	.130	.0000955		
P-461		3.1440	.2098	.02052	1.030	5,780	.01852	.05352	1.108	.474		.076	.225	.00188		
P-462		3.0829	.1193	.01144	1.032	3,355	.01077	.01807	1.062	.086		.035	.180	.000546		
621		9.4016	.5207	.1523	1.025	25,945	.08272	1.073	1.841	23.48		.260	.667	.0411	.528	.0391
623		9.5017	.4652	.1375	1.025	23,740	.07569	.8984	1.817	23.13		.250	.686	.0395	.522	.0339
624		9.3615	.5859	.1706	1.025	27,950	.08911	1.245	1.914	32.85		.283	.721	.0522	.569	.0451
626		9.3907	.4564	.1333	1.025	23,735	.07567	.8980	1.762	22.0		.249	.635	.0378	.531	.0349
643		9.3521	.4278	.1244	1.025	22,525	.07181	.8088	1.732	19.8		.236	.646	.0332	.515	.0301
645		9.3607	.3486	.1015	1.030	19,175	.06143	.5890	1.652	15.9		.216	.584	.0259	.481	.0239
646		9.2835	.4128	.1192	1.030	21,415	.06861	.7346	1.737	20.4		.229	.624	.0317	.522	.0279
SP-854	1100-0	7.7165	.4494	.1079	1.036	22,645	.07297	.8262	1.479	4.25		.342	.640	.07075		
SP-859		5.9175	.3287	.06050	1.030	14,740	.04722	.3480	1.281	1.5		.292	.505	.03705		
SP-901		3.3838	.7374	.07761	1.032	17,625	.05658	.4986	1.372	2.78		.326	.575	.0518		
SP-908		3.3607	.4869	.05090	1.030	12,920	.04139	.2674	1.230	1.5		.289	.470	.0292		
SP-909		8.4987	.3569	.09434	1.032	20,510	.06584	.6752	1.433	2.71		.332	.610	.0613		
613		9.1699	.4613	.1316	1.025	25,625	.08170	1.047	1.611	7.05		.362	.665	.0775		
614		9.2150	.4463	.1279	1.025	24,705	.07876	.9729	1.624	6.72		.356	.657	.0746		
615		8.7443	.4210	.1145	1.025	23,020	.07339	.8447	1.560	6.42		.341	.632	.0651		
616		8.7193	.3381	.09170	1.025	19,625	.06257	.6140	1.466	4.63		.315	.581	.0515		
617		8.7560	.2567	.06991	1.025	16,180	.05158	.4173	1.355	3.26		.289	.521	.0372		
618		8.7057	.2746	.07436	1.025	16,695	.05323	.4443	1.397	4.30		.295	.531	.0405		
619		9.1387	.5057	.1437	1.025	27,330	.08713	1.191	1.649	9.30		.375	.689	.0860		
SP-718	2024-T4	3.0024	.0800	.00747	.130	15,260	.00617	.0471	1.21	.613	.0625	.096	.203	.00182	.203	.00175
SP-719		3.0015	.0811	.00757	.130	15,500	.00627	.0486	1.21	.567		.095	.200	.00170	.204	.00163
SP-722		3.0564	.0997	.00948	.132	17,615	.00723	.0637	1.31	.917		.100	.220	.00223	.217	.00223
SP-848		3.3674	.1098	.01150	.137	20,470	.00872	.0892	1.32	1.10		.107	.225	.00264	.224	.00264
SP-849		3.0644	.0830	.00791	.137	15,380	.00655	.0504	1.21	.423		.087	.200	.00163	.191	.00158
SP-906		3.2238	.1284	.01288	.132	22,960	.00943	.108	1.37	1.50		.115	.265	.00347	.257	.00330
549		3.8473	.1280	.01532	.132	25,070	.0103	.129	1.49	1.48		.124	.253	.00386	.249	.00386
551		3.8463	.1248	.01493	.130	25,145	.0102	.128	1.46	1.70		.126	.273	.00408	.269	.00408
552		3.8434	.1177	.01407	.131	24,355	.00992	.121	1.42	1.50		.122	.258	.00383	.256	.00383
556		3.8475	.1410	.01687	.132	27,085	.0111	.150	1.52	1.79		.132	.281	.00460	.271	.00460
572		3.8504	.1434	.01717	.132	28,140	.0116	.163	1.48	2.20		.137	.283	.00496	.279	.00496
590		.30424	.6468	.006120	.132	12,090	.00496	.0300	1.23	.346		.081	.179	.00115		
593		.30549	.7660	$.7279\times10^{-2}$	.132	14,320	$.588\times10^{-2}$	.0421	1.24	.434		.095	.194	.00160	.194	.0016
606		.30616	.3710	.3533	.132	7,780	.319	.0124	1.11	.068		.055	.123	.000417		
608		.30663	.3995	.3810	.132	8,385	.344	.0144	1.11	.095		.058	.130	.000487		
610		.30696	.2859	.2730	.132	6,195	.254	.00787	1.07	.029		.046	.109	.000267		
561	1100-0	3.8787	.1272	1.535	.132	25,080	1.03	.129	1.49	.783		.168	.323	.00859		
573		3.8563	.1434	1.720	.132	27,000	1.11	.150	1.55	.906		.180	.327	.00939		
575		3.8764	.1424	1.717	.132	26,555	1.09	.145	1.58	.862		.173	.327	.00892		
576		3.8552	.1296	1.554	.132	25,790	1.06	.137	1.47	.851		.176	.321	.00899		
592		.32073	.5582	.5569	.132	11,710	.481	.0282	1.16	.088		.127	.211	.00298		
597		.33106	1.3480	1.388	.132	23,280	.956	.111	1.45	.708		.160	.313	.00752		
598		.33287	1.2700	1.315	.132	22,575	.927	.105	1.42	.701		.173	.304	.00812		
599		.33599	1.2080	1.262	.132	21,820	.896	.0978	1.41	.589		.154	.296	.00655		
600		.33265	.8641	.8941	.132	17,250	.708	.0611	1.26	.19		.128	.260	.00397		
601		.33079	.8125	.8360	.132	15,640	.642	.0502	1.30	.293		.144	.253	.00478		
602		.32665	1.0760	1.093	.132	19,315	.793	.0766	1.38	.428		.146	.282	.00550		

*NOTE: Targets too heavy for accurate determination of ΔM.

NASA-Langley, 1967 —— 32 A-897